Mean and Fluctuating Electron Density in Equilibrium Turbulent Boundary Layers

ANTHONY DEMETRIADES* AND RICHARD GRABOW†
Philco-Ford Corporation, Aeronutronic Division, Newport Beach, Calif.

A simplified analysis is used to predict the mean and fluctuating electron density profiles in equilibrium high-speed turbulent boundary layers. The analysis is based on the application of nonlinear statistics to equilibrium chemistry and experimentally determined turbulence characteristics. Closed-form solutions of the electron density fluctuations are obtained for typical statistical distribution functions of the gas temperature fluctuations. The temperature dependence of the electron density is determined from complete thermochemical equilibrium calculations and the results are fit to a form of the Saha equation. Results are presented for reacting turbulent boundary layers consisting of clean air, Teflon/air mixtures, and phenolic carbon/air mixtures. It is shown that the true mean electron density can be orders-of-magnitude greater than the value computed at the local mean temperature. In addition, the root-mean-square electron density fluctuation can greatly exceed the true mean value.

Nomenclature

B = exponent in Saha equation
C = constant in Saha equation
C_i = mass fraction of specie i
C_A = mass fraction of ablation products
E = ionization potential
h = static enthalpy
H = total enthalpy
H_T = total energy absorbed by ablating surface
k = Boltzmann constant
K_f = forward reaction rate
$\dot{m}$ = surface ablation rate
M_e = Mach number at edge of boundary layer
M_i = molecular weight of specie i
$n_e(\bar{T})$ = pseudoaverage electron density
$\langle n_e(T)\rangle$ = true mean electron density
$\Delta n_e(T)$ = rms electron density fluctuation
N = exponent of velocity profile power-law
P = static pressure
SDF = statistical distribution function
t = time
T = temperature
$\bar{T}$ = mean temperature
ΔT = rms temperature fluctuation
u = velocity
w = distribution function
Y = distance normal to surface
δ = boundary-layer thickness
γ = ratio of specific heats
ρ = density
τ_c = characteristic chemical relaxation time
χ = virtual fluctuation parameter

Subscripts

e = edge of boundary layer
W = wall
∞ = freestream

1. Introduction

THERE has recently been increased interest in the re-entry plasma sheath, and its effects upon communication, telemetry, and navigational functions. A significant portion of this interest has been devoted to the fluid dynamic and thermodynamic characteristics of the plasma sheath, particularly in the study of thin, highly ionized boundary layers. The turbulent boundary-layer problem is of particular interest since the re-entry turbulent flow regime is generally characterized by high ionization levels resulting from high temperature and the possible presence of alklai contaminants in the ablating surface. For high-speed flight, especially at the lower altitudes, it is current practice to compute the boundary-layer electron density using the local mean temperature and assuming thermochemical equilibrium conditions. The application of the equilibrium assumption is of course debatable, but a more important failing in these computations is to disregard the effect of the turbulent fluctuations on both the mean and the fluctuating electron density. The purpose of this paper is to demonstrate that, still within the equilibrium condition, this turbulence effect can be appreciable.

In a thermochemically equilibrated plasma the electron density fluctuations are driven primarily by the gas temperature fluctuations. The problem addressed here is to find the electron fluctuation once the temperature fluctuations are given. Generally, the electron behavior is statistically unusual because of the extremely nonlinear nature of its variation with temperature. Before showing the quantitative behavior of the electrons, their statistics can be illustrated with the aid of Fig. 1. Consider a temperature field fluctuating between T_1 and T_2, with mean value $\bar{T}$. Because of the steeply rising character of $n_e(T)$ the following become evident by inspecting Fig. 1: 1) the mean value $\langle n_e(T)\rangle$ of the electron density is higher than the "pseudoaverage" value $n_e(\bar{T})$, that is, the electron density computed at $\bar{T}$; and

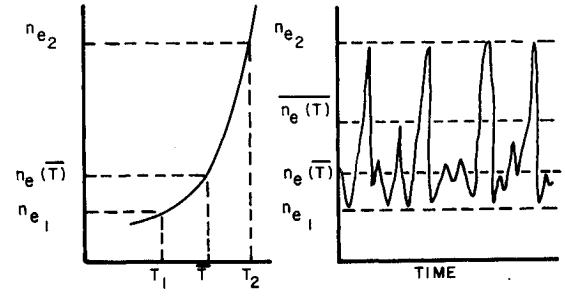

Fig. 1 Electron density time-history (right) and the fluctuation effect on the mean value (left).

Presented as Paper 70-743 at the AIAA 3rd Fluid and Plasma Dynamics Conference, Los Angeles, Calif., June 29–July 1, 1970; submitted August 13, 1970; revision received April 7, 1971.

* Supervisor, Experimental Aerodynamics Section. Associate Fellow AIAA.
† Supervisor, Aerodynamic Analysis Unit. Member AIAA.

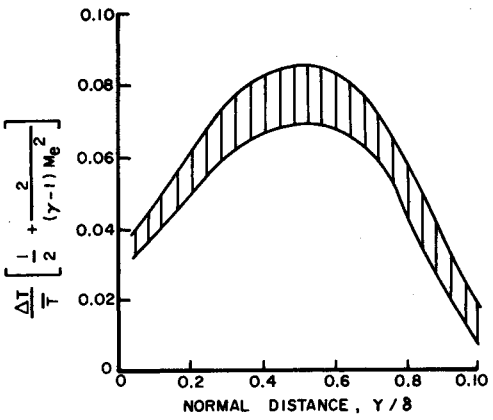

Fig. 2 Temperature fluctuation correlation from Kistler's data.[2]

2) the root-mean-square electron density fluctuation $\Delta n_e(T)$ can also be higher than the "pseudoaverage" value, $n_e(\bar{T})$.

In the following sections, a method of analysis for predicting $\langle\overline{n_e(T)}\rangle$ and $\Delta n_e(T)$ will be discussed. This method assumes that the temperature fluctuation ΔT is known, or can be predicted on the basis of experimental data.[1,2] For the present investigation, the data of Kistler[2] was utilized, and these results are reproduced in Fig. 2. The data band includes Mach numbers in the range, $1.7 \leq M_e \leq 4.7$, the effects of which are only partially correlated by the bracketed coefficient which tends to 0.5 at high Mach numbers. Thus, $\Delta T/\bar{T}$ approaches a maximum value of approximately 0.18 at $Y/\delta \simeq 0.5$. Although Kistler's data are considered to be the best available at supersonic adiabatic wall conditions, the present application of these data to reacting hypersonic boundary layers with heat and mass transfer is certainly questionable. Fortunately, the validity of this statistical analysis does not depend on the accuracy of the estimated temperature fluctuation, although the final electron density results are of course sensitive to the magnitude of the temperature fluctuations.

2. Statistical Theory

The statistical analysis used in this paper follows the procedure of Ref. 3. The moments of the probability function of the electron number density are determined for a given statistical distribution function (SDF) of the gas temperature and a given coupling relation between this temperature and the electron density. While a specific temperature SDF was chosen in Ref. 3, a number of such functions which relate more realistically to known turbulence behavior are chosen here. Vorticity and sound waves are not considered as electron producers in this analysis, and thermal ionization

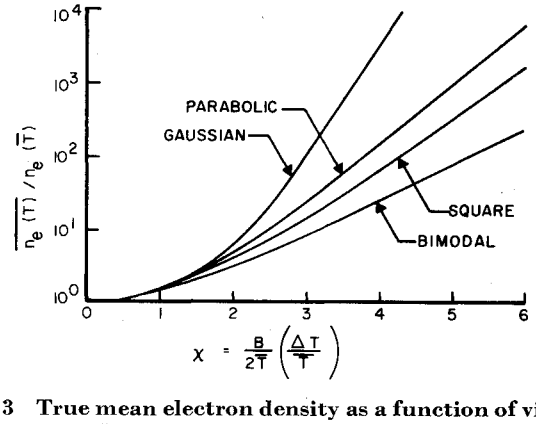

Fig. 3 True mean electron density as a function of virtual fluctuation parameter and SDF.

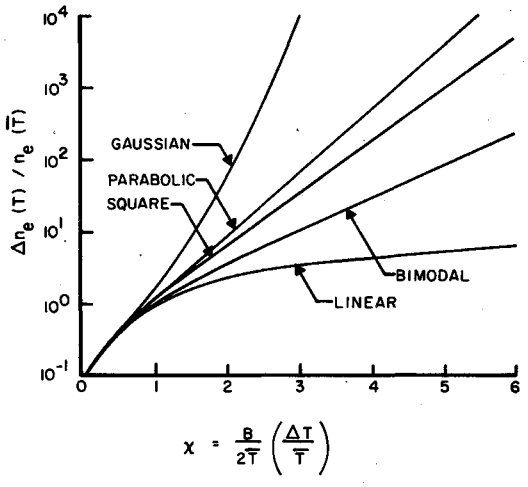

Fig. 4 RMS electron density fluctuation as a function of virtual fluctuation parameter and SDF.

as described by the Saha equation is assumed to be valid across the entire temperature range.

The electron densities can be computed from the relations[3]

$$\frac{\langle\overline{n_e(T)}\rangle}{n_e(\bar{T})} = 1 + \sum_{m=1}^{\infty} \frac{1}{m!}\left(\frac{B}{2\bar{T}}\right)^m \frac{\langle\overline{(\Delta T)^m}\rangle}{\bar{T}^m}$$

and

$$\frac{\Delta n_e(T)}{n_e(\bar{T})} = \left\langle \left\{ \frac{B}{2\bar{T}}\frac{\Delta T}{\bar{T}} + \sum_{m=2}^{\infty} \frac{1}{m!}\left(\frac{B}{2\bar{T}}\right)^m \left[\frac{(\Delta T)^m}{\bar{T}^m} - \frac{\langle\overline{(\Delta T^m)}\rangle}{\bar{T}^m}\right] \right\}^2 \right\rangle$$

It is important to realize that only in the linearized limit of $\langle\overline{(\Delta T)^m}\rangle = 0$, would the quantities $n_e(\bar{T})$ and $n_e(T)$ be identical. Since the quantity $B/2T \gg 1$, this limit is rarely attainable for realistic temperature fluctuations. In addition, for certain SDFs, the maximum contribution to the above expansions may come from the higher order terms.

For many statistical distribution functions of the temperature, the higher moments $\langle\overline{(\Delta T)^m}\rangle$ can be expressed in terms of the mean-square fluctuation $\langle\overline{(\Delta T)^2}\rangle$, in such a way that the preceding equations contain the dimensionless "virtual fluctuation" parameter

$$\chi = (B/2\bar{T})\Delta T/\bar{T}$$

where from here on, ΔT denotes the root-mean-square fluctuation. The results presented in this paper are based on Gaussian, parabolic, and square statistical distribution functions of the gas temperature; the "bimodal" distribution is also included from Ref. 3. Table 1 shows the higher moments of these distributions and the ratios

$$\langle\overline{n_e(T)}\rangle/n_e(\bar{T}) \text{ and } \Delta n_e(T)/n_e(\bar{T})$$

in terms of the "virtual fluctuation" parameter χ. Results are graphically presented in Figs. 3 and 4, where it is shown that these ratios can achieve rather large values. These magnitudes are a consequence of the extremely nonlinear electron density-temperature dependence. The effect of nonlinearity is especially pronounced for the Gaussian distribution because its probability is finite, although small, at temperatures far removed from the mean. The upper reaches of the Gaussian may contribute to unrealistically high values of $\langle\overline{n_e(T)}\rangle$ and $\Delta n_e(T)$ by admitting temperatures well above the freestream stagnation value, while the lower reaches of the Gaussian can admit negative absolute temperatures. It is possible to truncate the Gaussian distribution, but the resulting asymmetries greatly complicate the analysis. Also, at very low temperatures, the miniscule

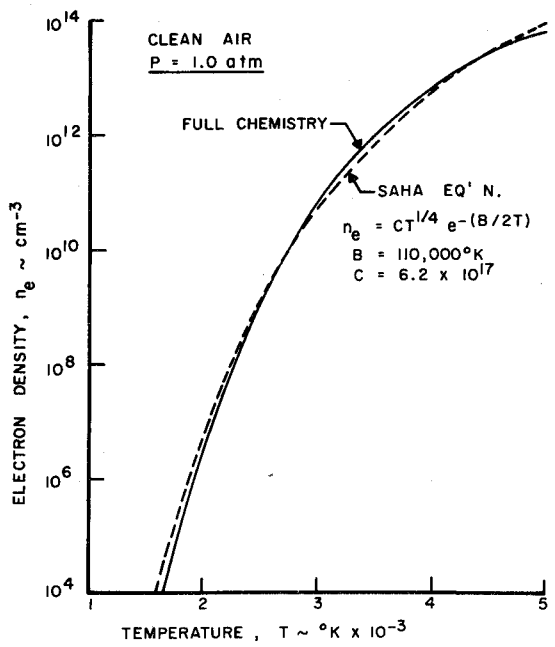

Fig. 5 Comparison between Saha equation and full chemistry solution for clean air.

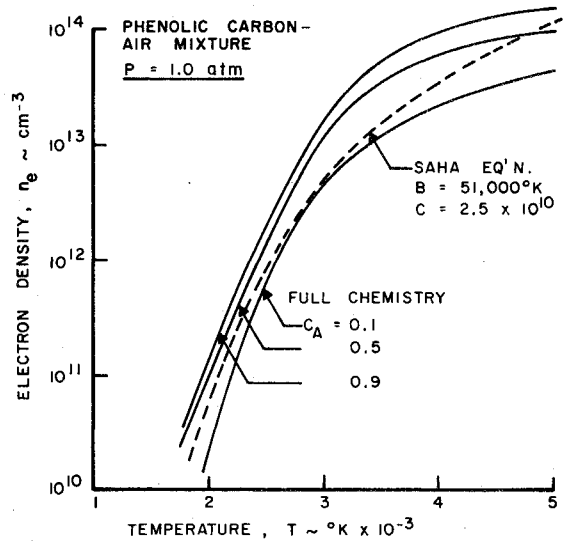

Fig. 6 Comparison between Saha equation and full chemistry solutions for phenolic carbon air mixture.

electron densities $n_e(\bar{T})$ resulting from thermal ionization drive the ratio $\langle n(T)\rangle/n(\bar{T})$ to large magnitudes, even for moderate values of $\Delta T/\bar{T}$. This result would be correct so far as thermal ionization at these temperatures is concerned, but in practical cases the nonthermal ambient electron density, however small, could modify the numerical results.

3. Chemistry Considerations

As discussed in Sec. 2, the present statistical approach requires a simple chemistry model to provide an algebraic relation between the instantaneous electron density and the thermodynamic variables. For the case where the flow is in thermochemical equilibrium, this relation exists in the form of the single-ionization Saha equation,

$$n_e = CP^{1/2}T^{1/4}e^{-B/2T} \quad \text{where } B = E/k$$

For the case of clean air ionization with a nitric oxide ionization potential, $E = 9.5$ ev, one obtains a value for $B = 110{,}000°K$. Some results of the Saha equation using this value are presented in Fig. 5, where a comparison is made with complete thermochemical equilibrium solutions. These calculations were performed with a computer code[4] that utilizes the most recent thermodynamic data for the determination of the minimum free-energy equilibrium condition. The comparison indicates excellent agreement over a relatively large temperature range, which partially justifies the use of the simplified Saha equation for the present statistical analysis. One should actually make this comparison for a larger temperature range since the statistical approach is based on temperature fluctuations integrated over their entire spectrum.

For the case of complex ionized gas mixtures, the Saha equation is assumed to apply if an effective value of B is utilized. This value is selected on the basis of complete thermochemical equilibrium solutions. To demonstrate this procedure, Fig. 6 presents the calculated electron density variations with temperature for varying mass fractions (C_A) of phenolic-carbon in air. The phenolic-carbon includes 100 ppm of sodium as a trace contaminant. To match these complete thermochemical equilibrium results with the Saha equation, an effective B value of 51,000°K is shown to be adequate.

Although the present investigation is limited to thermodynamically equilibrated boundary layers, it is important to at least indicate how the validity of this assumption should be tested. One possible approach would be to compare the characteristic time for chemical relaxation with a characteristic turbulence time. For clean air ionization, the critical chemical reaction is,

$$N + O \rightarrow NO^+ + e^-$$

Table 1 Typical symmetric statistical distribution functions of temperature fluctuations and resulting equilibrium electron densities

Type of distrib	Equation	Equation of mth central moment	$\Delta ne(T)/\overline{ne(T)}$	$\langle\overline{ne(T)}\rangle/ne(\bar{T})$
Gaussian	$w = \frac{1}{(2\pi)^{1/2}}\frac{1}{(\Delta T)}\exp-\left[\frac{(T-\bar{T})^2}{2(\Delta T)^2}\right]$	$(m-1)_{\text{odd}}!(\Delta T)^m$; $m = 2, 4, \ldots$ e.g., $M_2 = (\Delta T)^2$ $M_4 = 1 \times 3(\Delta T)^4$ $M_6 = 1 \times 3 \times 5 \times (\Delta T)^6$	$(e^{\chi^2} - 1)^{1/2}$	$e^{\chi^2/2}$
Square	$w = 0$ for $(\bar{T} - a) > T > (\bar{T} + a)$ $w = \frac{1}{2}a$ for $(\bar{T} - a) < T < (\bar{T} + a)$ where $a = (3)^{1/2}(\Delta T)$	$\frac{[(3)^{1/2}]^m}{m+1}(\Delta T)^m$, even m	$[(3)^{1/2}\chi \coth(3)^{1/2}\chi - 1]^{1/2}$	$\frac{\sinh(3)^{1/2}\chi}{(3)^{1/2}\chi}$
Parabolic	$w = [3/4(5)^{1/2}]1/(\Delta T) \times [1 - (T - \bar{T})^2/5(\Delta T)^2]$		$\{(5\chi^3/6(5)^{1/2})[2(5)^{1/2}\chi \times \cosh^2(5)^{1/2}\chi - \sinh^2(5)^{1/2}\chi] \times [(5)^{1/2}\chi \cosh(5)^{1/2}\chi - \sinh(5)^{1/2}\chi]^2 - 1\}^{1/2}$	$[3/5(5)^{1/2}\chi^3][(5)^{1/2}\chi \times \cosh(5)^{1/2}\chi - \sinh(5)^{1/2}\chi]$
Bimodal	$w = \frac{1}{2}\{\delta[T - (\bar{T} + (\Delta T))] + \delta[T - (\bar{T} - (\Delta T))]\}$	$(\Delta T)^m$, even m	$\tanh\chi$	$\cosh\chi$

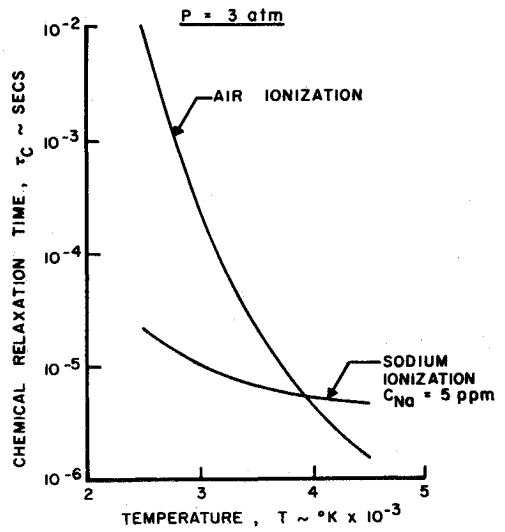

Fig. 7 Characteristic chemical relaxation times.

and the forward reaction rate[5] is,

$$K_f = 6.4 \times 10^9 T^{1/2} e^{-32400/T} [\text{cm}^3/(\text{g-mole})\text{-sec}] (T \text{ in } ^\circ\text{K})$$

From the Law of Mass Action, the production rate of nitric oxide ions is,

$$(d/dt)(C_{NO^+}) = K_f \rho (M_{NO^+}/M_O M_N) C_O C_N (\rho \text{ in g/cm}^3)$$

Defining the chemical relaxation time as

$$\tau_c \equiv (C_{NO^+})_{equil}/(d/dt)(C_{NO^+})$$

and assuming that the oxygen and nitrogen atoms have attained equilibrium values, the chemical relaxation time is,

$$\tau_c = (1/K_f \rho)(M_O M_N/M_{NO^+})(C_{NO^+}/C_O C_N)_{equil}$$

For complex gas mixtures on ablating bodies, it is usually quite difficult to select a single reaction as the basis for the characteristic relaxation time. However, if sodium contaminants provide the major contribution to the total ionization, then it is likely that the critical reaction will be the ionization of sodium atoms by collision with oxygen atoms[6]

$$Na + 2O \rightarrow Na^+ + e^- + O_2$$

with a forward reaction rate,

$$K_f = 4 \times 10^6 \text{cm}^6/(\text{g-mole})^2 - \text{sec}$$

Applying the mass action law yields the chemical relaxation time

$$\tau_C = (M_O^2/K_f \rho^2)(C_{Na^+}/C_{Na} C_O^2)_{equil}$$

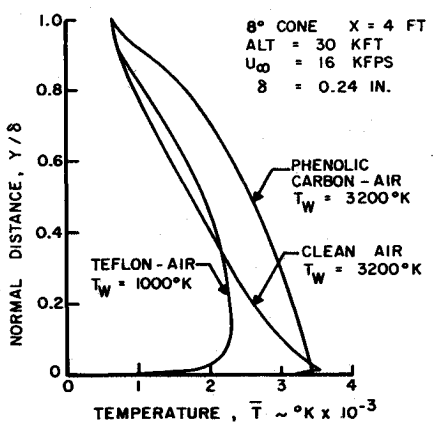

Fig. 8 Mean temperature profiles for various gas mixtures.

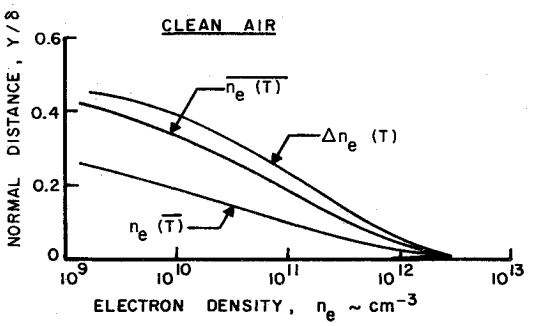

Fig. 9 Electron density profiles for clean air—parabolic SDF.

Typical values of the characteristic chemical relaxation times for clean air and sodium ionization are presented in Fig. 7. These results were computed at a pressure of 3 atm (flight condition of Sec. 5). The results indicate that the equilibrium assumption may be more valid for sodium ionization since the relaxation times for air ionization are relatively long, particularly at low temperatures.

It would be desirable to compare the curves of Fig. 7 with turbulence times indicative of the mixing or decay of the turbulence pattern. In principle, equilibrium will prevail in those regimes where these times are considerably greater than the chemical times. The proper definition of the turbulence time is however in some doubt. The integral time scale of the moving pattern (the time scale of the so-called optimum autocorrelation[7]) would appear to be a suitable characteristic turbulence time, but this scale has not been measured under conditions of high Mach number and temperature. When such experimental information is available definite boundaries might be set on the applicability of the equilibrium boundary-layer calculations and the improvements shown herein.

4. Boundary-Layer Analysis

To compute the fluctuation effects on boundary-layer electron density profiles, the mean temperature ($\bar{T}$) and pseudo average electron density, $n_e(\bar{T})$ profiles through the boundary layer are initially determined. In the present investigation, an approximate method is used to predict these profiles in a hypersonic turbulent boundary layer that is experiencing ablation effects. The major assumptions in this analysis are: 1) zero pressure gradient and constant wall temperature; 2) power-law velocity profiles in which the exponent is a function of the known ablation rate; 3) unity Prandtl and Lewis numbers for all species, thus permitting the use of the Crocco relations for enthalpy and species mass fraction profiles; and 4) use of thermochemical equilibrium solutions for

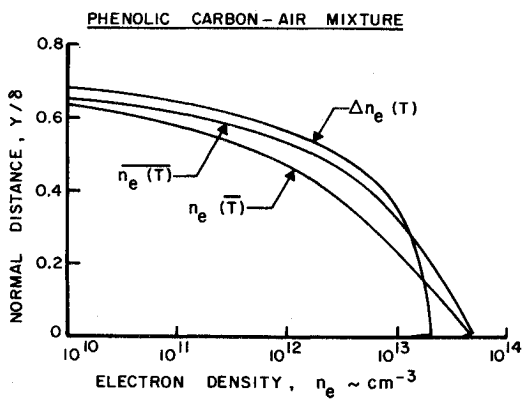

Fig. 10 Electron density profiles for phenolic carbon/air mixture—parabolic SDF.

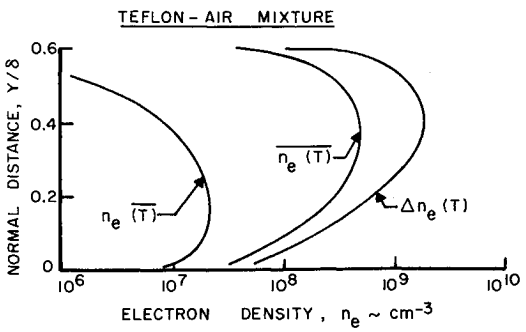

Fig. 11 Electron density profiles for Teflon/air mixture—parabolic SDF.

computed pressure, enthalpy, and element mass fraction at each point in the boundary layer.

The specific relations employed in the analysis are

$$u/u_e = (Y/\delta)^{1/N}$$

$$C_{A_W} = \frac{1}{1 + H_T/(H_e - h_W)} \text{ where } h_W = h_W(P,T_W,C_{A_W})_{\text{equil}}$$

$$h = h_W + (H_e - h_W)u/u_e - (H_e - h_e)(u/u_e)^2$$

$$C_A = C_{A_W} + (C_{A_e} - C_{A_W})u/u_e$$

$$\bar{T} = \bar{T}(P,h,C_A)_{\text{equil}} \text{ and } n_e(\bar{T}) = n_e(P,h,C_A)_{\text{equil}}$$

The next step in the boundary-layer analysis is to determine the profile of the rms temperature fluctuation ΔT. Since this quantity cannot presently be theoretically determined, it is necessary to utilize existing experimental data. For this investigation, the data of Kistler (reproduced in Fig. 2) are used, although they were obtained under lower Mach number conditions with zero heat and mass transfer. These temperature fluctuation results are utilized in conjunction with the computed mean temperatures and the effective B values from the Saha equation (Sec. 3) to determine the virtual fluctuation parameter χ. The final step in the boundary-layer analysis involves the utilization of χ in Figs. 3 and 4 to determine the true mean electron density, $\langle n_e(T) \rangle$ and the rms electron density fluctuation $\Delta n_e(T)$. This step also involves the selection of the proper statistical distribution function (SDF) of the temperature fluctuations. At the present time there is insufficient experimental data to justify any particular one of the four SDFs considered herein. For the majority of the results presented in the following section, the parabolic SDF has been selected.

5. Results for a Typical Flight Condition

The pseudoaverage, true mean, and rms fluctuating electron density profiles have been computed for the following

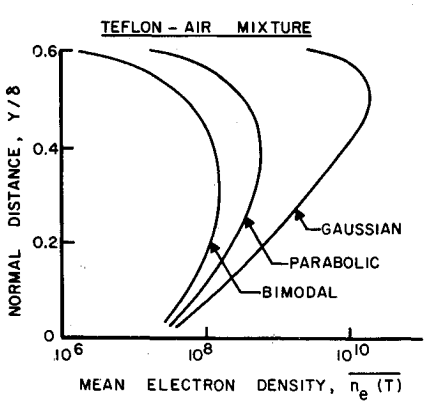

Fig. 12 Effect of SDF on true mean electron density for a Teflon/air mixture.

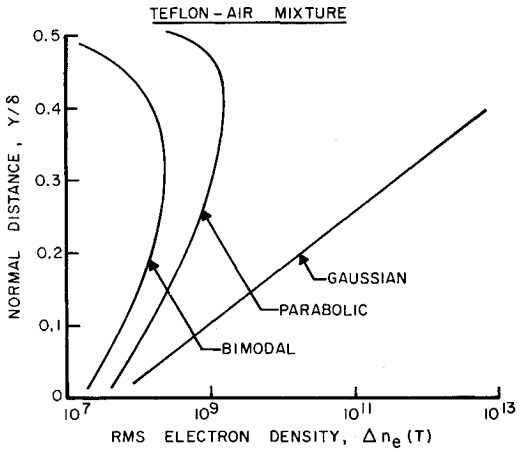

Fig. 13 Effect of SDF on rms electron density fluctuation for a Teflon/air mixture.

re-entry configuration and flight condition: a pointed 8° half-angle cone flying at a speed of 16,000 fps at an altitude of 30,000 ft. The profiles were evaluated at the 4-ft station for various surface conditions: ablating Teflon (T_W = 1000°K), ablating phenolic carbon (T_W = 3200°K), and a nonablating surface (T_W = 3200°K). The mean temperature profiles are presented in Fig. 8 where it is shown that the phenolic carbon/air mixture experiences the highest temperatures throughout most of the boundary layer. This is attributed to predominately exothermic reactions, whereas the Teflon/air mixture experiences highly endothermic reactions. The dissociated clean air profile has the highest peak temperature, but the temperatures rapidly decrease as a function of normal distance from the surface. For each of the gas mixtures, the pseudoaverage, true mean, and rms electron densities are presented in Figs. 9–11, assuming a parabolic SDF.

It is interesting to note the trend and magnitude differences between the results for the various gas mixtures. Since the same $\Delta T/\bar{T}$ profile is used for all cases, the differences are due to variations in $\bar{T}$, $n_e(\bar{T})$, and B. However, the more important result is the indication that the true mean and rms fluctuation electron densities can be orders of magnitude greater than the pseudoaverage electron density computed at mean temperature. This enormous effect is even more pronounced in Figs. 12 and 13 for the case of the Teflon-air mixture. Included in these two figures are the less severe results obtained by assuming a bimodal SDF. These comparisons clearly demonstrate the importance of the selected SDF and the need for sufficient experimental data to permit a valid selection.

6. Conclusions

The present analysis of mean and fluctuating electron density profiles in equilibrium turbulent boundary layers has led to the following conclusions:

1) The true mean electron density $\langle n_e(T) \rangle$ and the rms electron density fluctuation $\Delta n_e(T)$ can both exceed the pseudo average electron density $n_e(\bar{T})$ by orders-of-magnitude.

2) The mean and fluctuating electron densities are dependent on the assumed temperature fluctuations which for the present investigation have been determined from limited experimental data.

3) Predictions of mean and fluctuating electron density are shown to be quite sensitive to the value of the "virtual fluctuation" parameter (χ) and the assumed statistical distribution function (SDF).

4) The modified Saha equation provides an adequate representation of equilibrium ionization for use in the present analysis.

5) The assumption of thermodynamic equilibrium for the analysis of fluctuation effects is more applicable at very high temperatures.

6) The application of this method of analysis for re-entry flight conditions requires an estimate of the temperature fluctuation magnitudes, statistical distribution function, and optimum autocorrelation which are presently not available from experimental measurements.

References

[1] Wallace, J., *Hypersonic Turbulent Boundary Layer Measurements Using an Electron Beam*, NASA SP-216, Dec. 10–11, 1968, p. 255.

[2] Kistler, A., "Fluctuation Measurements in a Supersonic Turbulent Boundary Layer," *The Physics of Fluids*, Vol. 2, No. 3, 1959, p. 290.

[3] Demetriades, A., "Electron Fluctuations in an Equilibrium Turbulent Plasma," *AIAA Journal*, Vol. 2, No. 7, July 1964, pp. 1347–1349; also Lane, F. and Zeiberg, S. L., "Comment on 'Electron Fluctuation in an Equilibrium Turbulent Plasma,'" *AIAA Journal*, Vol. 3, No. 5, May 1965, pp. 989–990.

[4] Kubert, B., "The Computation of the Products of Chemical Reactions in Equilibrium," TR U-1721, 1961, Philco-Ford, Calif.

[5] Bortner, M., "A Review of Rate Constants of Reactions in Re-entry Flow Fields," T15 R685D13, June 1968, General Electric.

[6] Kane, J., "Nonequilibrium Sodium Ionization in Laminar Boundary Layers," *AIAA Journal*, Vol. 2, No. 9, Sept. 1964, pp. 1651–1653.

[7] Favre, A., "Review of Space-Time Correlations in Turbulent Fluids," *Journal of Applied Mechanics*, June 1965, p. 241.

AUGUST 1971 AIAA JOURNAL VOL. 9, NO. 8

Fluid Mechanics of Train-Tunnel Systems in Unsteady Motion

MIKLOS SAJBEN*
California Institute of Technology, Pasadena, Calif.

The dynamic characteristics of bodies moving in long, finite channels are studied using a one-dimensional, incompressible fluid description. It is shown that the motion of the body and the fluid contained in the channel are closely and nonlinearly coupled and therefore an understanding of the system dynamics requires consideration of both body and fluid. The nonsteady inertial aspects of the motion may be important in many practical situations. The character of the solution is investigated using phase plane methods. The findings are compared with numerically integrated solutions yielding body and fluid speeds, as well as drag coefficients. The effects of various initial body speeds are studied. Compressibility effects are estimated and found to be slight for present systems. The theory includes steady-state operation as a singular case.

Nomenclature

c_D = drag coefficient
D = drag force on body
f = friction coefficient
F = propulsive force
k_j = loss coefficients defined in Eq. (18), j = 1 to 5
l = body length
L = channel length
m_j = loss coefficients defined in Eq. (24), j = 3 to 5
M = body mass; Mach number
p = static pressure
P = propulsion power
r = radial coordinate
R = channel or body radius
Re = Reynolds number
t = time
u = air velocity
U = mean air velocity
V = body velocity
x = coordinate along channel axis
X = body position coordinate
β = U/V velocity ratio
ϕ = $(\kappa_c/\kappa_b)^{1/2}$
γ = ratio of specific heats
Δ = distance of near field boundary from parallel section of body
ν = kinematic viscosity
κ = loss coefficient
λ = characteristic length
ψ = $L\rho R_c^2\pi/M$, air to body mass ratio
ρ = fluid density
σ = $(R_b/R_c)^2$, blockage ratio
ξ = axial coordinate in coordinate system fixed to body
ζ = loss coefficient

Subscripts

b = body
c = channel
cr = critical
e = exit
f,F = locations deffned on Fig. 2
0 = inlet
r,R = locations defined on Fig. 2
1,2 = locations defined on Fig. 1
$*$ = steady-state

Superscripts

$\pm$ = $U \gtrless 0$
$\hat{}$ = modified value (Eqs. 12, 27, and 33)

Presented as Paper 70-141 at the AIAA 8th Aerospace Sciences Meeting, New York, January 19–21, 1970; submitted August 12, 1970; revision received April 28, 1971. The author wishes to express his appreciation to B. Dayman, Jr., and to T. Kubota for numerous interesting discussions and useful comments on this subject. The interest and support of L. Lees is gratefully acknowledged.

* Presently Associate Scientist at McDonnell Douglas Research Laboratories, St. Louis, Mo. Member AIAA.

1. Introduction

SUBWAY systems presently under consideration are intended to employ higher speeds and higher traffic densities than systems in operation today. Both factors tend to aggravate problems of aerodynamic nature: the additional power requirement due to air drag is higher, the heat released